BIO-OPTICS FOR OCEAN COLOR REMOTE SENSING

OF THE BLACK SEA

(Black Sea Color)

TN15: Ocean color algorithms cross-comparison

Workpackage:	*4*	
Author(s):	*V. Slabakova*	*IO-BAS*
	Prof. S. Moncheva	*IO-BAS*

1. Objectives

The report aims to inter-compare the OLCI standard and regional bio-optical algorithms for estimation of chlorophyll a (CHL), diffuse attenuation coefficient at 490 nm K_d (490), Total Suspended Matter (TSM) and absorption coefficient by non-pigmented particles and colored dissolved organic matter at 443 nm (ADG443) in the Black Sea

2. Materials and methods

Sentinel 3 OLCI ocean color products (CHL, K_d (490), TSM and ADG443) retrieved from regional (see for details TN14) and standard algorithms (EUMETSAT, 2018) were cross-compared along two transect located between Bulgarian -Romanian (43°37'N, 30°37'E) and Bulgarian – Turkish (42°03'N, 30 °03'E) borders (Fig. 1).

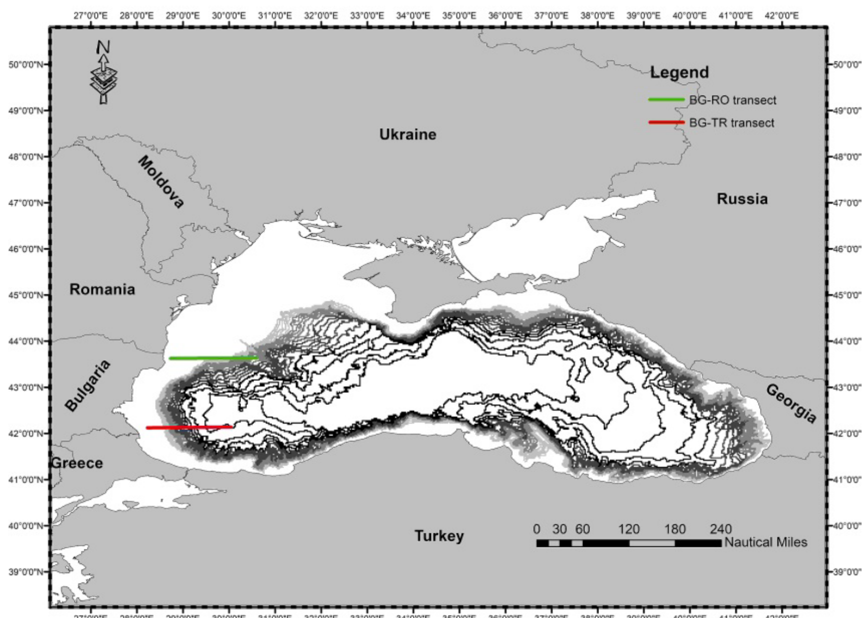

Figure 1. Transects from which OLCI ocean color products (CHL, K_d(490), TSM and ADG443) retrieved from regional and standard algorithms were extracted

The locations of transects were selected to represent the Black Sea waters with different bio-optical features. The Bulgarian –Romanian (BG-RO) transect spanned more complex bio-optical waters, largely perturbed by the Danube waters, while Bulgarian – Turkish (BG-TR) transect represented the relatively clear meso-oligotrophic Black Sea waters. Values of specific ocean color product were extracted along each transect from S3A/OLCI Level 2 Full Resolution image acquired on 24.05.2017 (S3A_OL_2_WFR____20170524T081032_20170524T081232_20171109T021621_0119_018_078__MR1_R_NT_002). The OLCI scene was downloaded from EUMETSAT Data Centre (https://archive.eumetsat.int/usc/). The regional ocean color products were computed from atmospherically corrected OLCI L2 water-leaving reflectances (ρ_w, dimensionless), which were converted into R_{rs} dividing them by π, applying the equation with corresponding coefficients of the specific bio-optical algorithm (see for details TN14). Inter-comparison of ocean color algorithms were summarized using scatter plots and by tabulating the R^2, slope and intercept from linear regression of matching retrievals along given transect. In order to evaluate spatial differences in algorithm performance the maps of ocean color products were generated and compared.

2. OLCI CHL products cross-comparison

A comparison of OLCI CHL products derived from regional (BS_CHL, TN#14) and global algorithms CHL_OC4ME (Morel et al.,2007) and CHL_NN (Doerffer &Schiller, 2007) along BG-RO and BG-TR transects using OLCI data acquired on 24th May 2017 is presented in Figure 2 and Table 1. For these two transects, there are 1075 data points; for coincident BS_CHL, CHL_OC4ME and CHL_NN data. Comparison between BS_CHL and CHL_OC4ME explained 98.5% of the variance in the data with intercept close to 0, but a high slope (2.94 and 4.64 respectively for BG-RO and BG-TR transects). There is a large offset between the algorithms at both low (< 1mg.m^{-3}) and high (>1 mg.m^{-3}) CHL concentrations. For BS_CHL and CHL_NN, only 6% of variance between the two algorithms is explained on the BG-RO transect. There is a large scatter and offset between the two algorithms over the entire BS_CHL range (0.2-1.52 mg.m-3). Comparison between CHL_OC4ME and CHL_NN on the BG-RO transect explained 11% variance in the data, the slope is low (0.27), the intercept is relatively high (1). Offset and scatter between the algorithms are large (Fig 1-A). Relatively good correlation between the datasets are presented for CHL_OC4MEvsCHL_NN (R^2=0.65) and BS_CHLvsCHL_NN (R^2 =0.70) on the BG –TR transect, but with high slopes and negative intercepts.

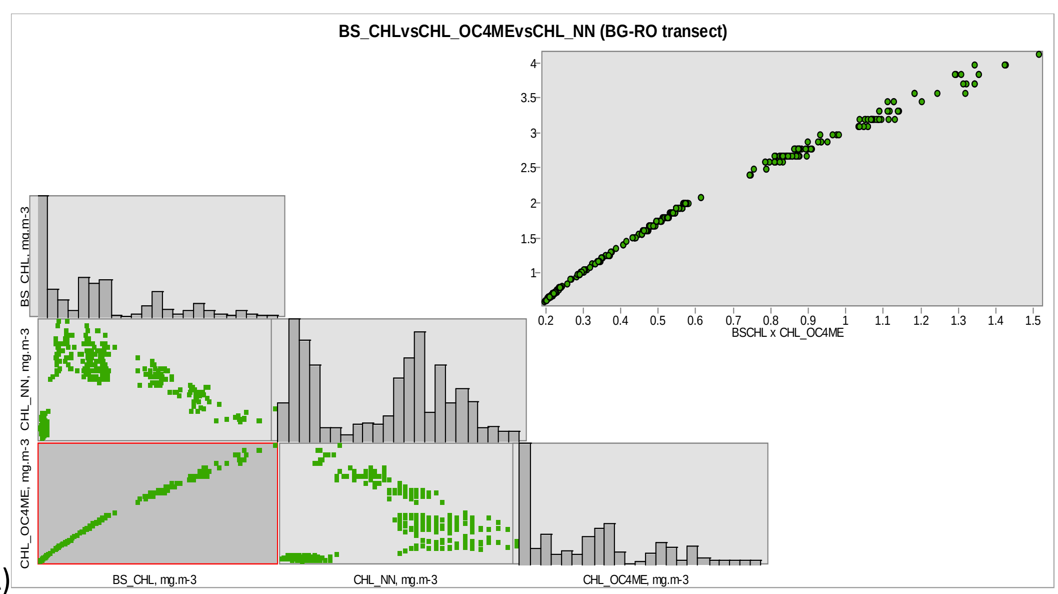

A)

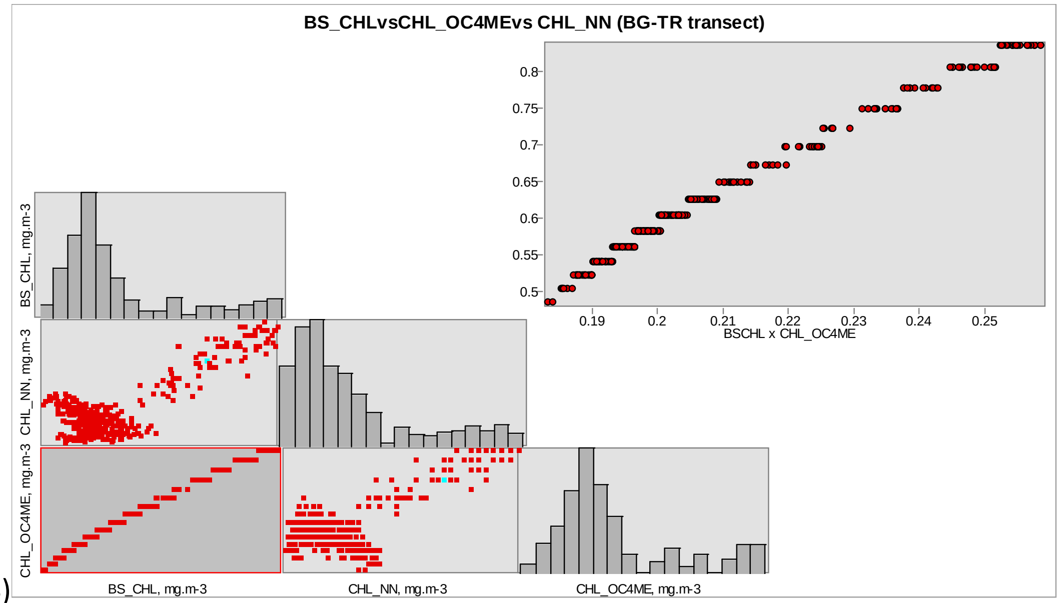

B)

Figure 2. Scatter plot matrixes of OLCI BS_CHL, CHL_OC4ME and CHL_NN (A for BG-RO transect and B)BG-TR transect (see Fig. 1 for details of transects)

Table 1.Percentage variance explained (R^2), intercept and slope from linear regression between BS_CHL, CHL_ OC4Me and CHL_NN chlorophyll *a* along BG-RO and BG-TR transects

	R^2	Slope	Intercept	R^2	Slope	Intercept
	BG-RO transect (N=544)			BG-TR transect (N=531)		
BS_CHL vs CHL_OC4ME	0.98	2.94	0.13	0.99	4.63	-0.34
BS_CHL vs CHL_NN	0.06	0.85	1.75	0.70	44.25	-7.88
CHL_OC4ME vs CHL_NN	0.11	0.27	1	0.65	9.18	-4.4

The spatial differences between the CHL algorithms are illustrated in satellite images generated from OLCI Level 2 data acquired on 24th May 2017 (Fig. 3). BS_CHL and OC4ME algorithms reproduce but with different magnitude (BS_CHL< CHL_OC4ME) the broad patterns that would be associated with CHL distribution in the Black Sea during spring season i.e., increased values in high-chlorophyll areas (North western Black sea and coastal regions) and lower concentrations in the shelf and central offshore Black Sea regions. By contrast, CHL_NN exhibited the higher values of CHL in the Bulgarian and Turkish coastal and shelf waters as well as in the open Black Sea which is unusual pattern of CHL distribution in the Black Sea. However the salient point of this figure is the large difference in predictions among the algorithms, as expected from the statistical results obtained from validation exercises presented in TN17.

A)
B)
C)

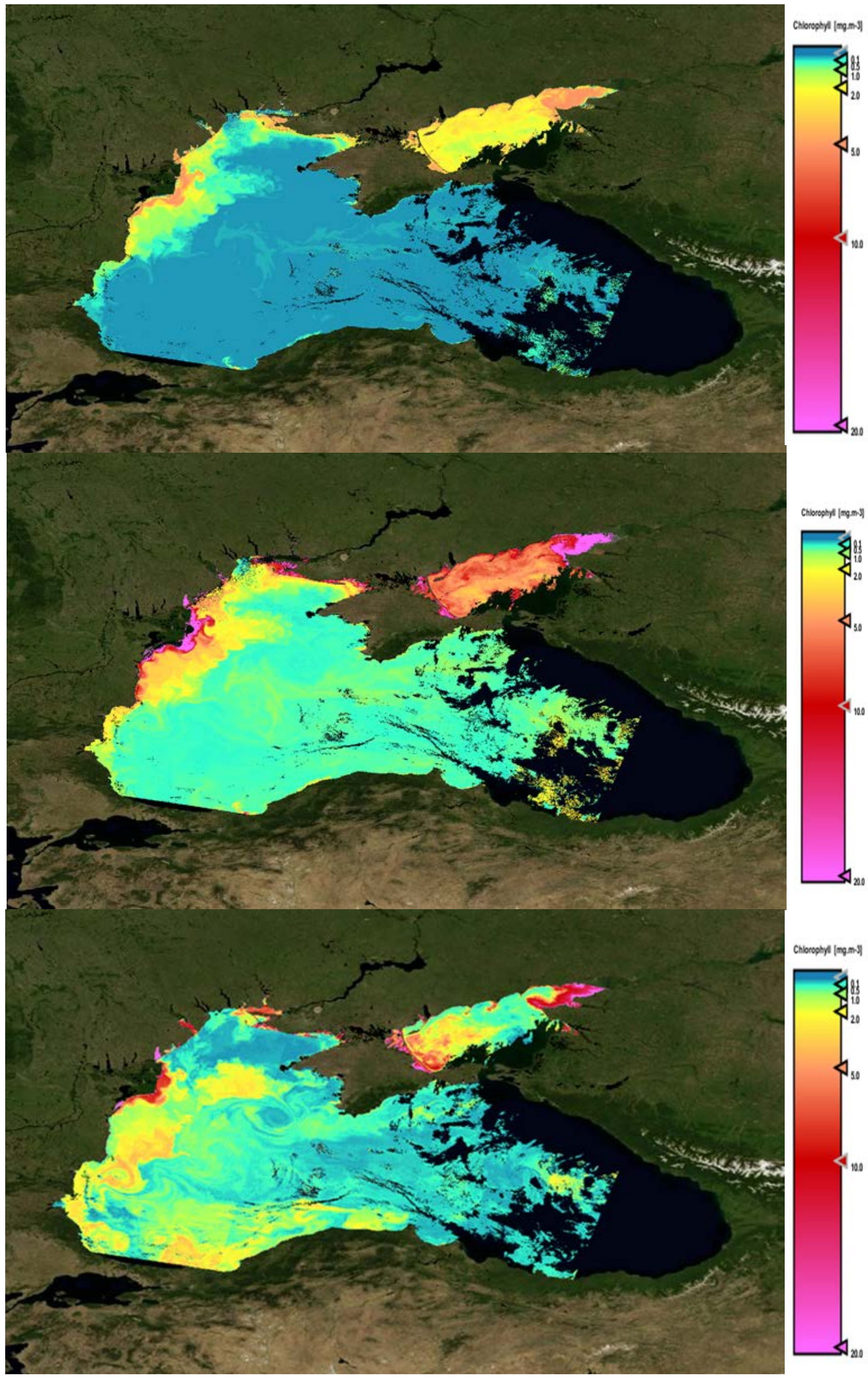

Figure. 3 Comparison of OLCI CHL products for 24th May 2017 using: A)BS_CHL, B)CHL_OC4ME and C)CHL_NN algorithms

To highlight the spatial variability in the satellite images between the algorithms, CHL values are extracted from BG-RO and BG-TR transects (Fig 4). The profiles of BS_CHL and CHL_OC4ME CHL values generally have a similar shape for both transects, but CHL concentrations derived from OC4ME algorithm are 3 times higher than BS_CHL. CHL_NN overestimates the pigment concentrations and the spatial trends are erratic with large oscillations between high and low CHL values over small spatial scales.

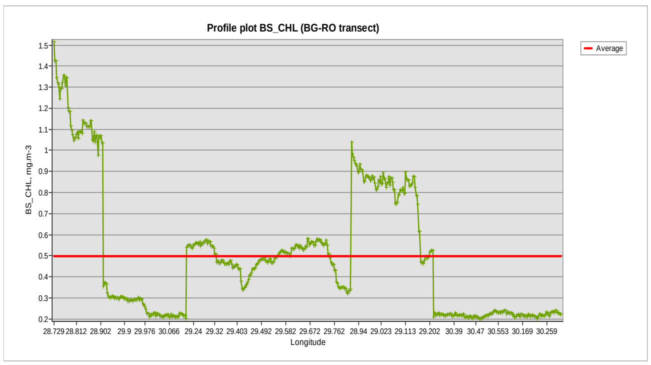

A)

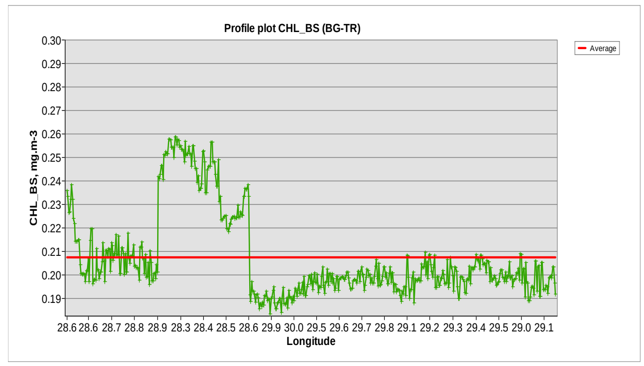

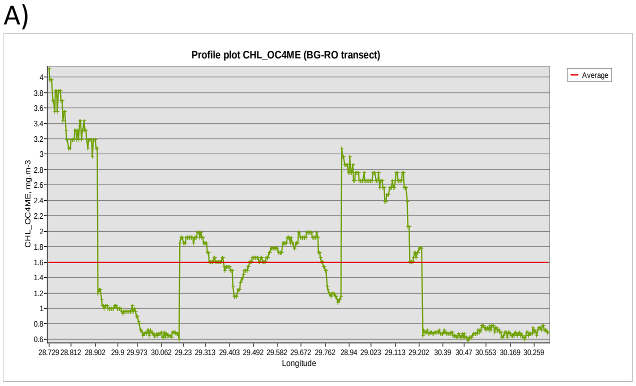

B)

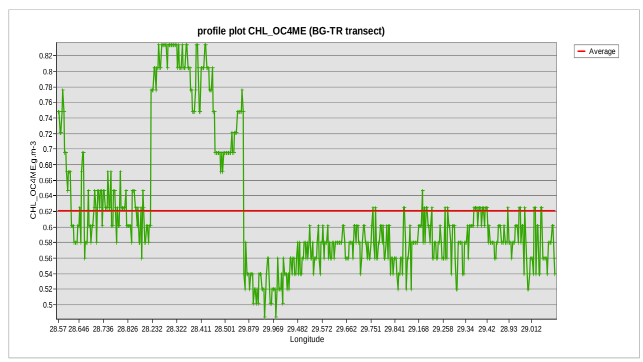

E)

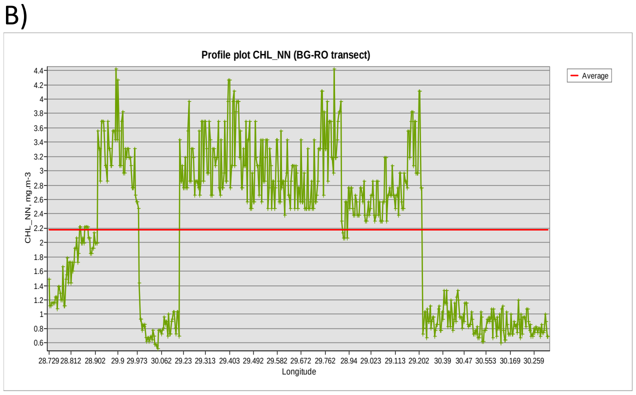

C)

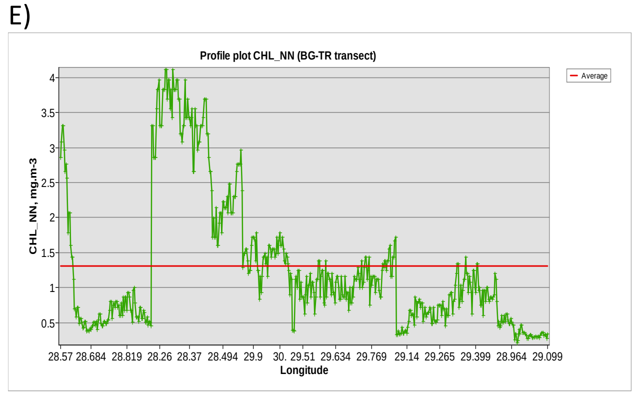

F)

Figure 4. Comparison of OLCI CHL products for 24th May 2017 along BG-RO transects (A) BS_CHL, (B) CHL_OC4ME, (C) CHL_NN, and for the BG-TR transect (D) BS_CHL, (E) CHL_ OC4ME, (F) CHL_NN

3. OLCI Diffuse Attenuation Coefficient at 490nm $K_d(490)$ products cross-comparison

A comparison of OLCI $K_d(490)$ products derived from regional ($K_d(490)$_BS, TN#14) and global (Kd490_OLCI -OK2-560, Morel et al.,2007) algorithms along BG-RO and BG-TR transects using OLCI data acquired on 24th May 2017 is presented in Figure 5 and Table 2. For these two transects, there are 1075 data points for coincident $K_d(490)$_BS and $K_d(490)$_OLCI data.

For both transects the results of comparison between Kd(490)_BS and Kd(490)_OLCI diffuses attenuation coefficient at 490 nm explained high correlation between datasets (0.99 for BG-RO transect and 0.98 for BG-TR transect). The estimated slope of the regression line is lower (0.72) for the BG-RO transect than for the BG-TR transect that is close to 1.

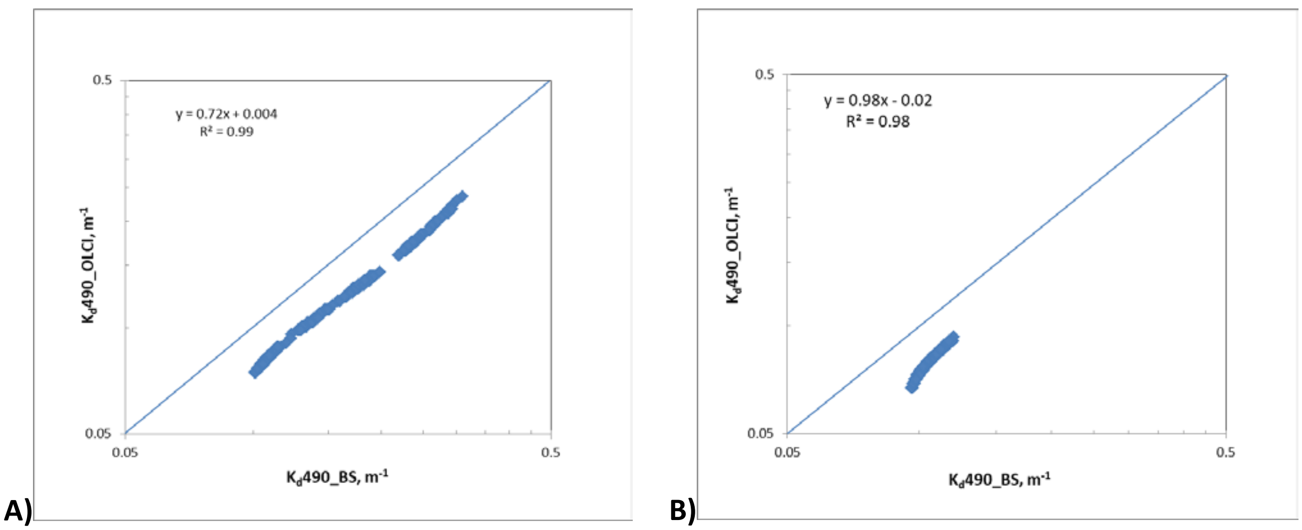

Figure 5.Scatter plots of $K_d(490)$_BS vs $K_d(490)$_OLCI: A) for BG-RO transect and B) for BG-TR transect

Table 2.Percentage variance explained (R^2), intercept and slope from linear regression between $K_d(490)$_BS and $K_d(490)$_OLCI diffuse attenuation coefficient at 490 nm along BG-RO and BG-TR transects

	R^2	bias	Intercept	R^2	Slope	Intercept
	BG-RO transect (N=544)			BG-TR transect (N=531)		
$K_d(490)$_BS vs $K_d(490)$_OLCI	0.99	0.72	0.0041	0.98	0.98	-0.02

The spatial differences between the OLCI $K_d(490)$ algorithms are illustrated in satellite images generated from OLCI Level 2 data acquired on 24th May 2017 (Fig.3). Generally, the $K_d(490)$ values retrieved by both algorithms have good spatial consistency. $K_d(490)$_BS and $K_d(490)$_OLCI algorithms reproduce the patterns that would be associated with $K_d(490)$ distribution in the Black Sea during spring season i.e., increased values (North western Black Sea area which is strongly influenced by Danube, Dnieper and Dniester rivers discharge and coastal regions) and lower concentrations in the shelf and central Black Sea regions. However, there are some notable differences between K_d490 values estimated by the different algorithms. Global algorithm produces estimates that are generally lower relative to the regional, particularly at high K_d490 values which is consistent with the statistical results obtained from the matchup analyses (sea details in TN#17).

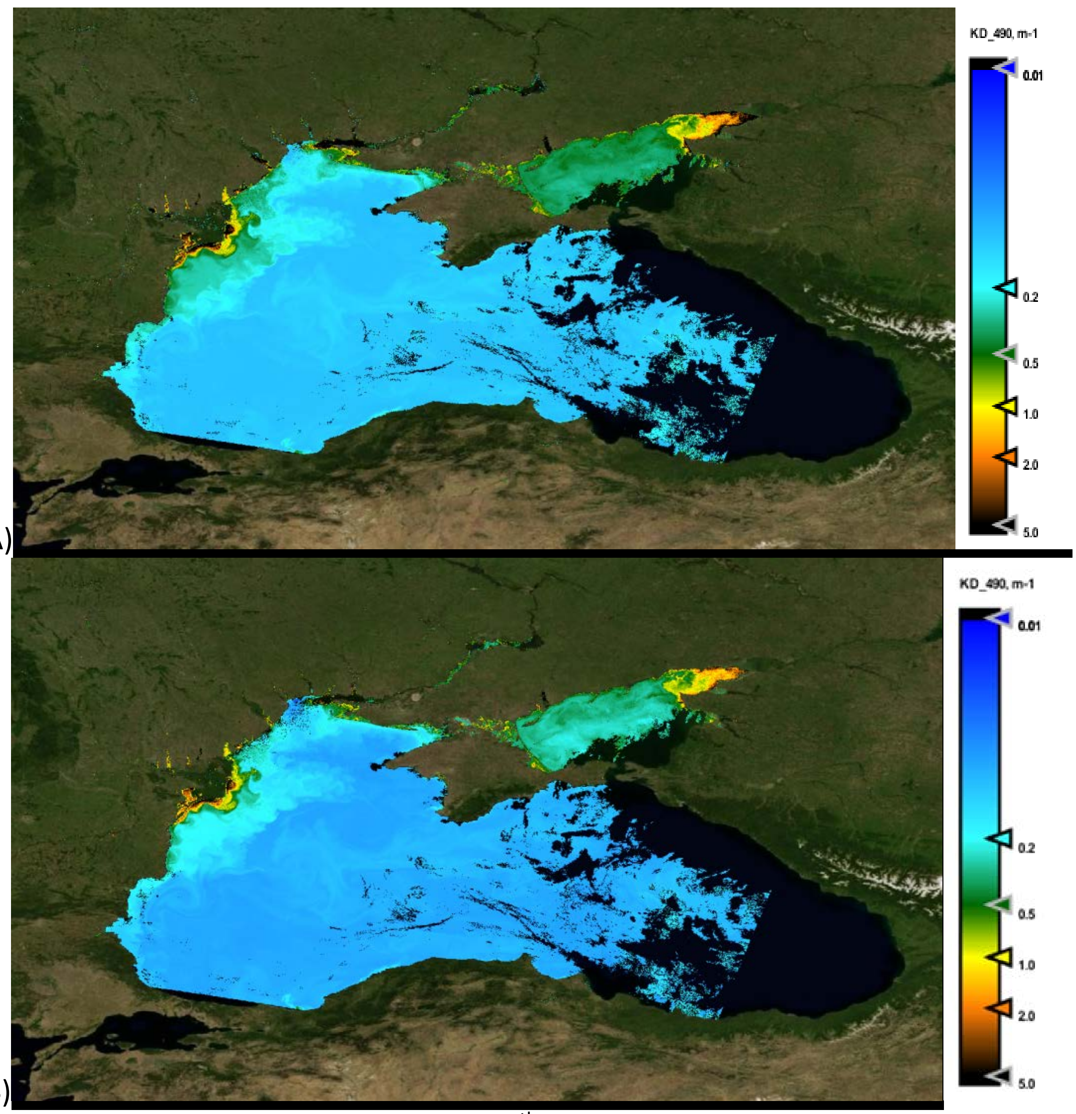

A)
B)

Figure 6. Comparison of $K_d(490)$ products for 24th May 2017 using: A)$K_d(490)$_BS, B) $K_d(490)$_OLCI algorithms

To point out the spatial variability in the satellite images between the algorithms $K_d(490)$ values are extracted from BG-RO and BG-TR transects (Fig 7). For both transects the shape of $K_d(490)$ profiles derived from regional and global algorithms are comparable. The standard OLCI $K_d(490)$ algorithm underestimate the $K_d(490)$ values with 25% comparing to the regional algorithm. For BG-RO transect the mean $K_d(490)$ values derived from $K_d(490)$_BS and $K_d(490)$_OLCI algorithms are respectively 0.166 $m^{-}1$ and 0.124 m^{-1} while for the clear Black Sea waters represented by BG-TR transect they are with 40% lower.

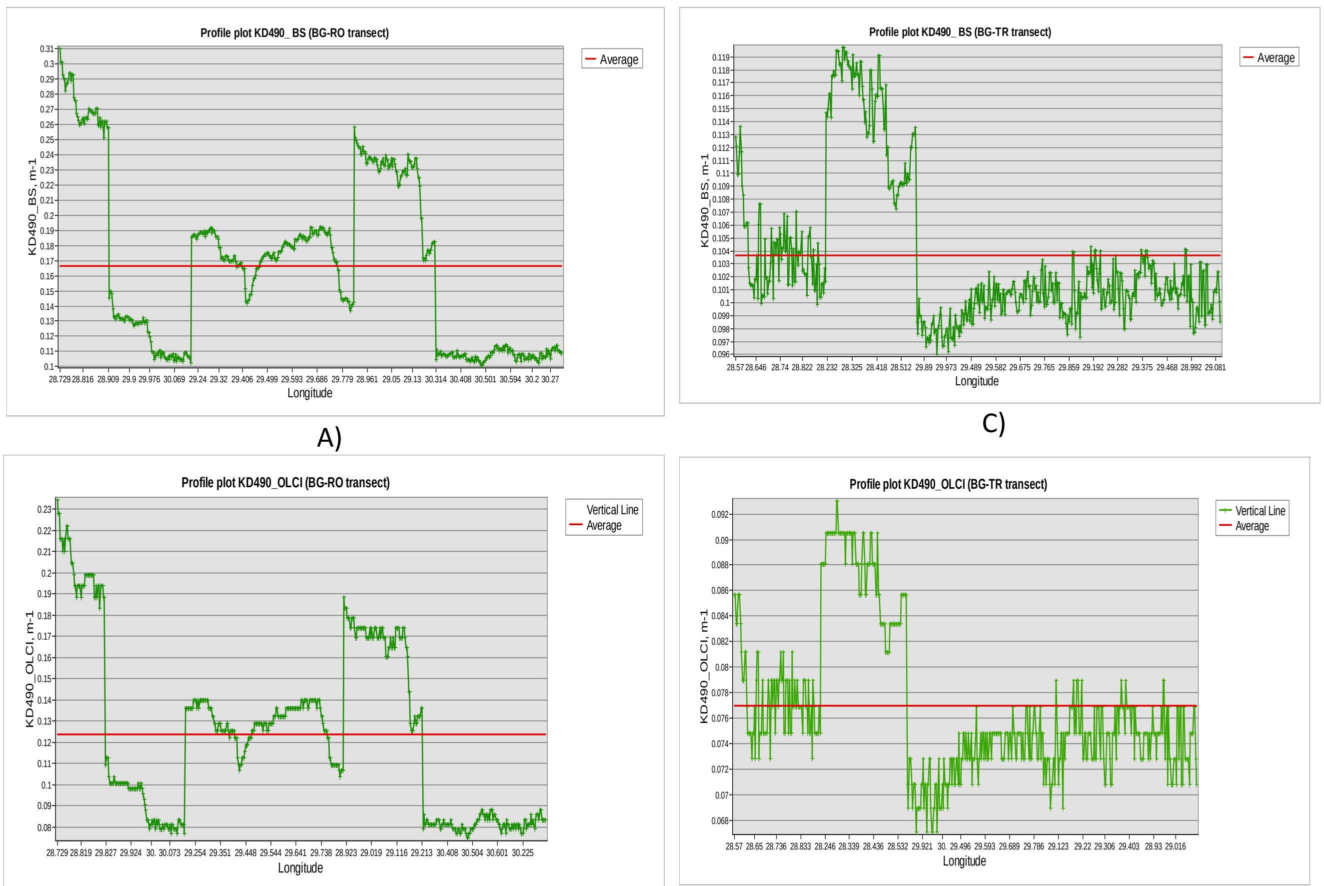

A) C) B) D)

Figure 7. Comparison of $K_d(490)$ products for 24th May 2017 along BG-RO transects (A) $K_d(490)$_BS, and (B) $K_d(490)$_OLCI and for the BG-TR transect (C) $K_d(490)$_BS, and (D) $K_d(490)$_OLCI.

4. OLCI absorption coefficient by non-pigmented particles and colored dissolved organic matter at 443 nm (ADG 443 nm) cross – comparison

A comparison of OLCI ADG443 products derived from regional (ADG443_BS, TN#14) and global (ADG443_NN, Doerffer &Schiller, 2007) algorithms along BG-RO and BG-TR transects using OLCI data acquired on 24th May 2017 is presented in Figure 8 and Table 3. For these two transects, there are 1075 data points for coincident ADG443_BS and ADG_NN data. Comparison between ADG443_BS and ADG443_NN explained 68% and 62% of the variance in the data respectively for BG-RO and BG-TR transects. The intercepts of the regression lines for both transects are close to 0 but the slopes are high (Tab. 3).

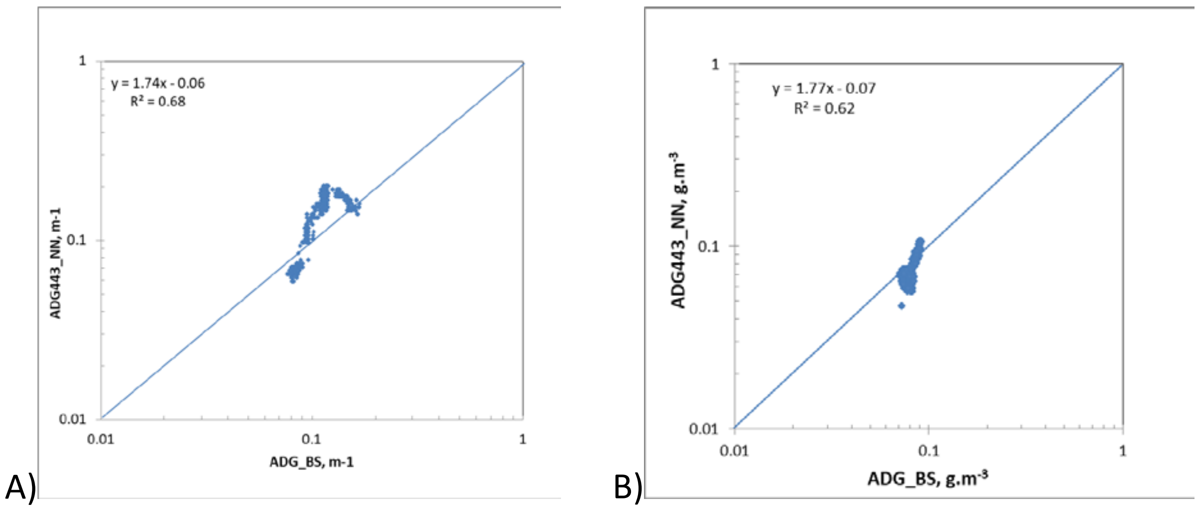

Figure 8.Scatter plots of ADG443_BS vs ADG443_NN: A) for BG-RO transect and B) for BG-TR transect

Table 3.Percentage variance explained (R^2), intercept and slope from linear regression between ADG443_BS and ADG443_NN along BG-RO and BG-TR transects

	R^2	Slope	Intercept	R^2	Slope	Intercept
	BG-RO transect (N=544)			BG-TR transect (N=531)		
ADG443_BS vs ADG443_NN	0.68	1.74	-0.06	0.62	1.77	-0.07

The spatial differences between the OLCI ADG443 algorithms are illustrated in satellite maps produced from OLCI Level 2 data acquired on 24th May 2017 (Fig.9). Generally, the AGD443 values retrieved by both algorithms have good spatial consistency. However, there are some differences between the ADG443 estimated by the different algorithms. Global algorithm underestimates at low ADG44 values relative to the regional, whilst at high concentrations its estimates are generally higher than ADG443_BS. This trend of the global algorithm is also confirmed in comparison of the ADG443 profiles extracted form BG-RO and BG-TR transects (Fig.10). For the both transects, global algorithm overestimated at high ADG443 values and underestimated at low ADG443 values comparing to the regional. Its spatial trends are erratic with large oscillations between high and low ADG443 values over small spatial scales.

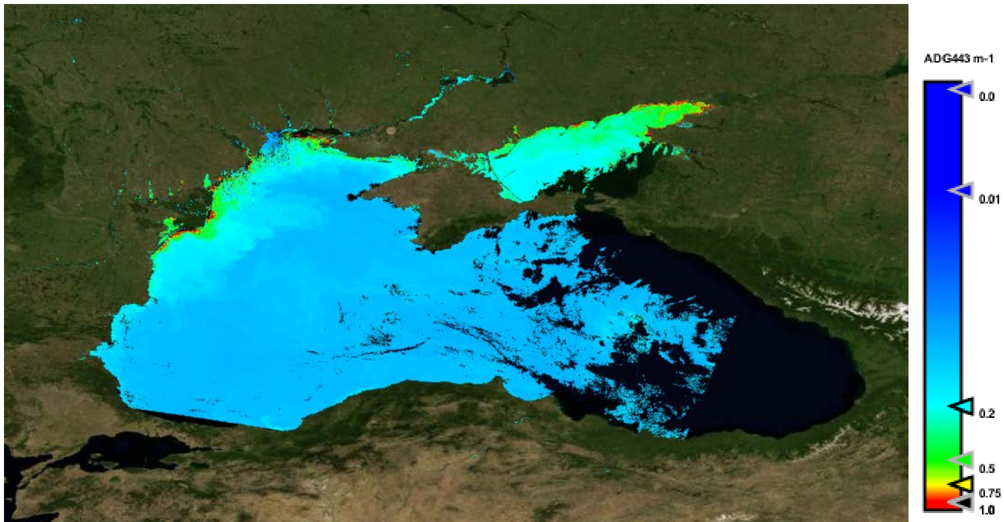

A)

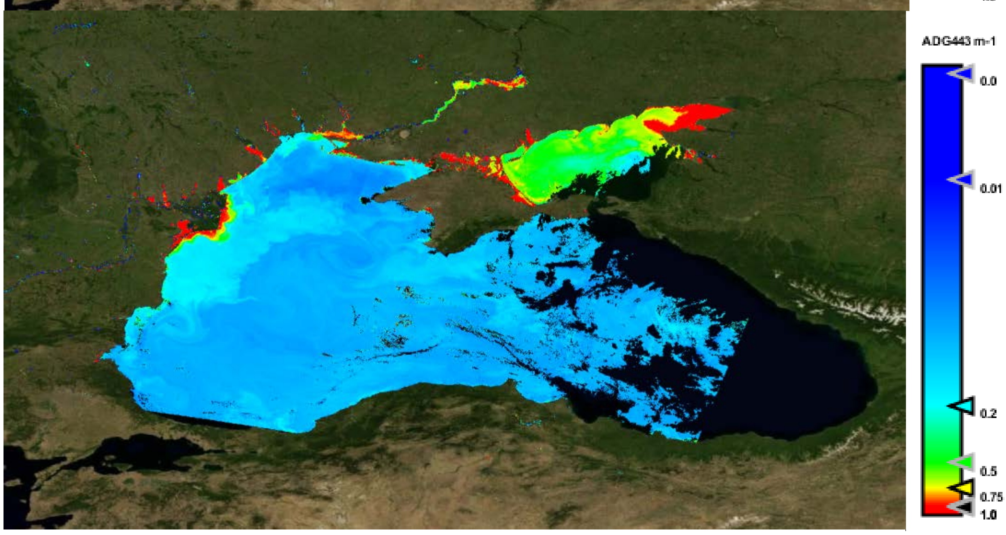

B)

Figure 9. Comparison of OLCI ADG443 products for 24th May 2017 using: A)ADG443_BS and B) ADG443_NN algorithms

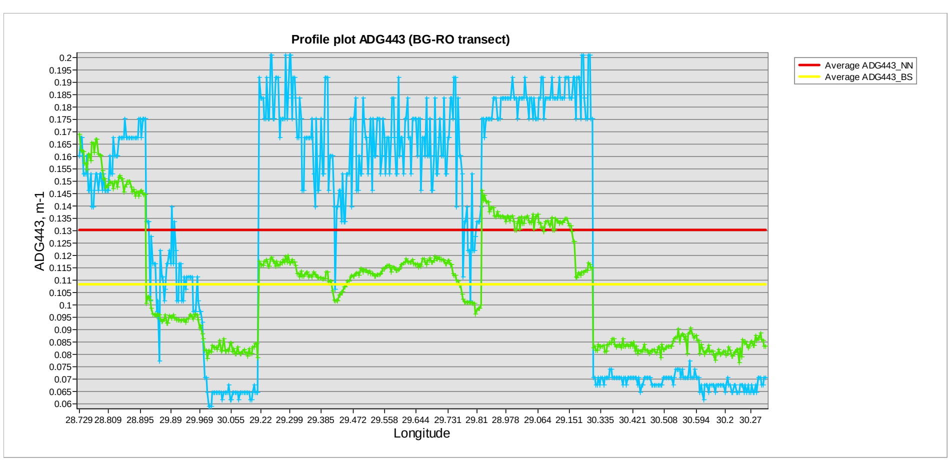

A)

B) 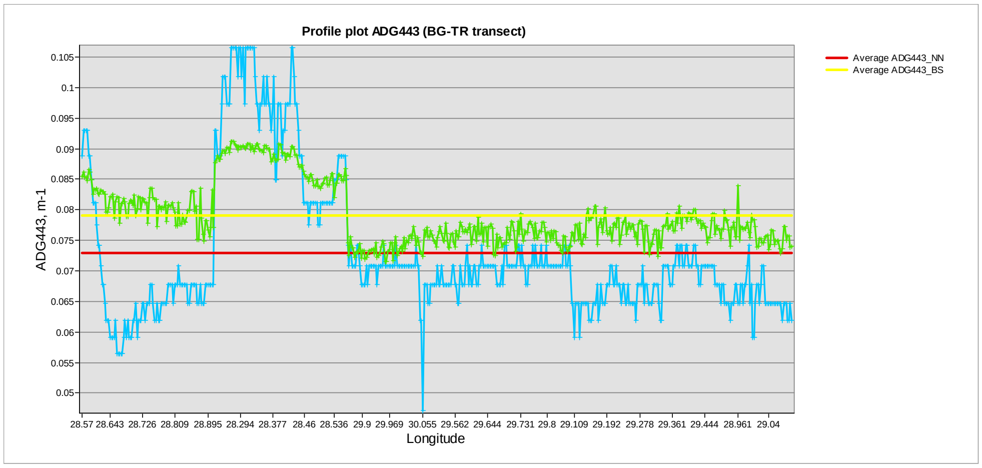

Figure 10. Comparison of OLCI ADG443 products for 24th May 2017 along BG-RO transects (A) and BG-TR transect (B). Green line correspond to the ADG443 values derived from regional algorithm (ADG443_BS) and blue line from the global (ADG_NN)

5. OLCI Total Suspended Matter (TSM) products cross-comparison

A comparison of OLCI TSM products derived from regional (TSM_BS, TN#14) and global (TSM_NN, Doerffer &Schiller, 2007) algorithms along BG-RO and BG-TR transects using OLCI data acquired on 24th May 2017 is presented in Figure 11 and Table 4. For these two transects, there are 1075 data points for coincident TSM_BS and TSM_NN data.

For BG-RO transect a weak linear correlation (R^2=0.29) between TSM data derived from regional and standard OLCI TSM algorithms is obtained whereas for the BG-TR transect there is no correlation between TSM_BS and TSM_NN data. Offset between the algorithms is large for the both transects.

A) 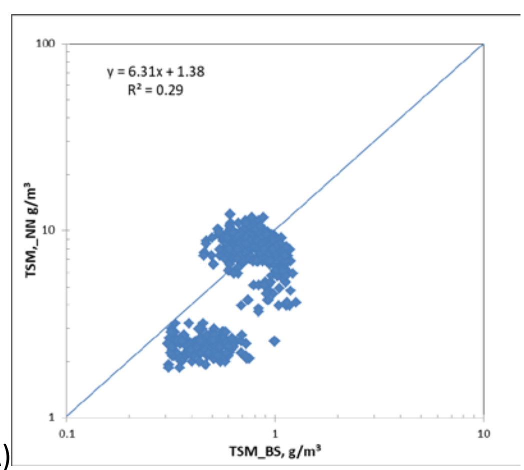

B) 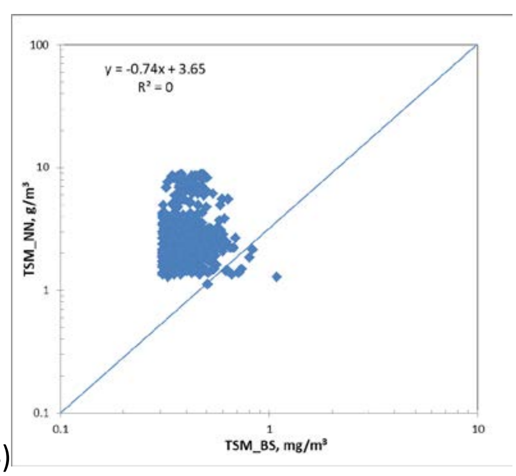

Figure 11. Scatter plots of TSM_BS vs TSM_NN: A) for BG-RO transect and B) for BG-TR transect

Table 4. Percentage variance explained (R^2), intercept and slope from linear regression between TSM_BS and TSM_NN along BG-RO and BG-TR transects

	R^2	Slope	Intercept	R^2	Slope	Intercept
	BG-RO transect (N=544)			BG-TR transect (N=529)		
TSM_BS vs TSM_NN	0.29	6.31	1.38	0.001	0.74	3.65

The spatial differences between the OLCI TSM algorithms are illustrated in satellite maps produced from OLCI Level 2 data acquired on 24th May 2017 (Fig.12). The salient point of this figure is the large variance in predictions of TSM concentrations among the algorithms. TSM_NN algorithm produces estimates that are significantly higher relative to regional algorithm. It exhibited the higher values (>8 g/m^3) of TSM in the Romanian, Bulgarian and Turkish coastal and shelf waters while the TSM_BS algorithm produce increased TSM concentrations in North western Black Sea which could be associated with Danube , Dnieper and Dniester rivers plumes.

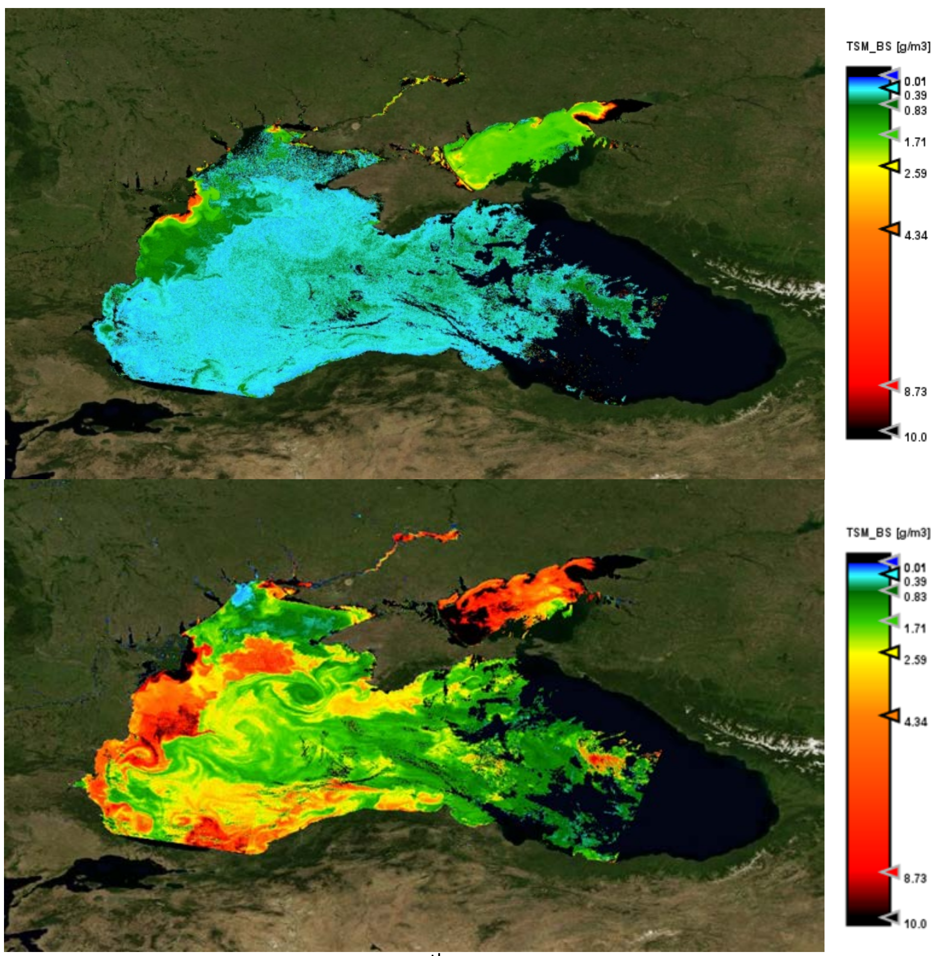

B)

Figure 12. Comparison of OLCI TSM products for 24th May 2017 using: A) TSM_BS and B) TSM_NN algorithms

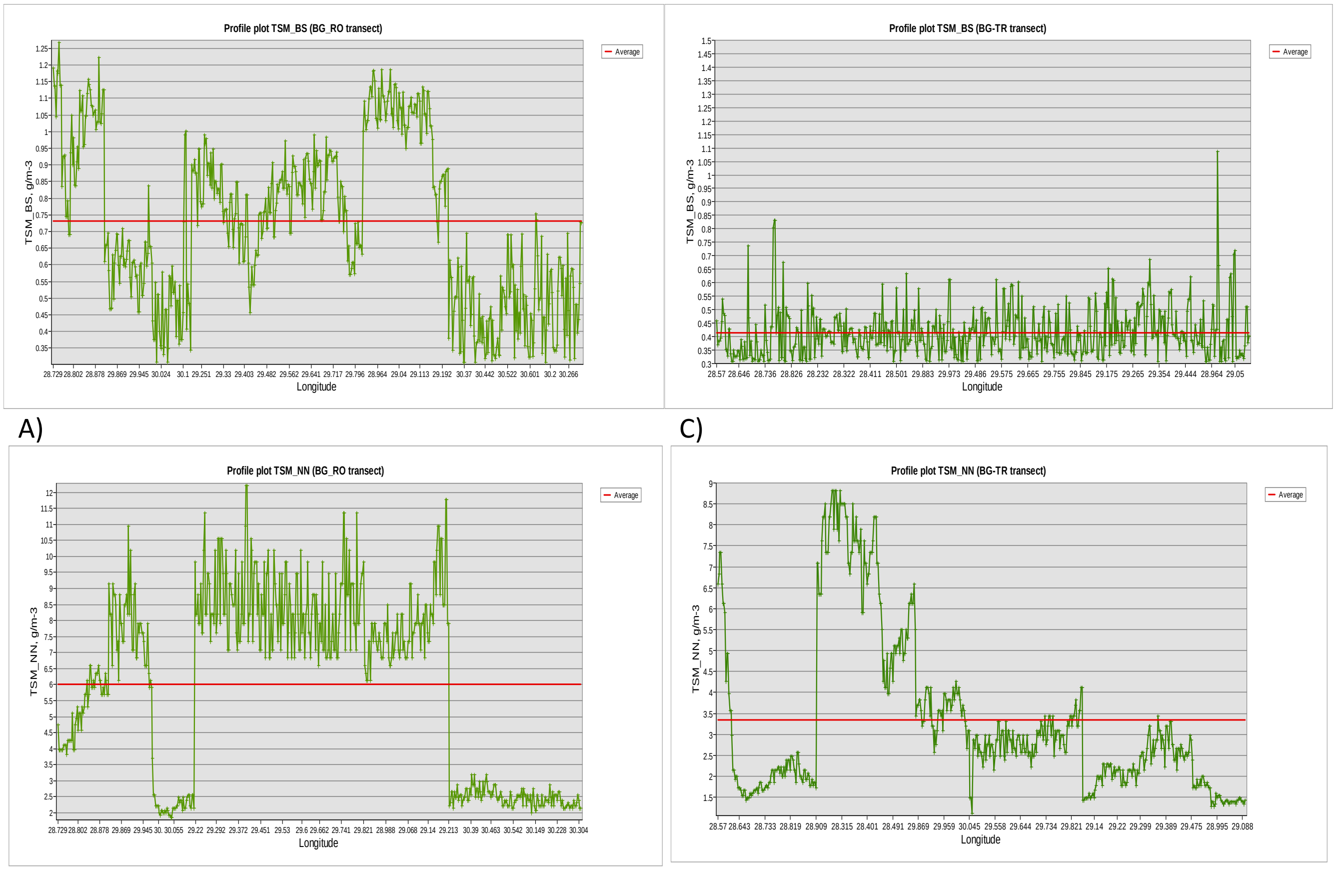

A) C) B) D)

Figure 13. Comparison of OLCI TSM products for 24th May 2017 along BG-RO transects (A) TSM_BS, and (B) TSM_NN and for the BG-TR transect (C) TSM_BS and (D) TSM_NN

To highlight the spatial variability in the satellite images between the algorithms TSM values are extracted from BG-RO and BG-TR transects (Fig 13). For both transects, the shape of TSM profiles extracted from regional and global algorithms are divergent. For BG-RO transect the regional algorithm produce the highest TSM values in the coastal area while the global in the shelf. For BG-TR transect, the global algorithm shows large oscillations between high and low TSM values in contrary to the regional which produced negligible fluctuations with significantly smaller amplitudes. For both transects the TSM concentrations derived from global algorithm are about 90% higher than regional.

5. Conclusions

The cross-comparison of OLCI ocean color products indicates:

- BS_CHL and OC4ME algorithms reproduce but with different magnitude the broad patterns that would be associated with CHL distribution in the Black Sea during spring season.

- Global (CHL_NN and OC4ME) algorithms significantly overestimate CHL consternations in comparison to the BS_CHL algorithm
- Global K_d(490) algorithm produces estimates that are generally lower relative to the regional, particularly at high K_d490 values.
- Global and regional K_d(490) algorithms reproduce the patterns that would be associated with K_d(490) distribution in the Black Sea during spring season.
- Global ADG443_NN algorithm underestimates at low ADG443 values relative to the regional, whilst at high concentrations its estimates are generally higher than ADG443_BS.
- The AGD443 values retrieved by regional and global algorithms have a good spatial consistency
- TSM_NN algorithm produces estimates that are significantly higher relative to regional algorithm.
- Large spatial variance in reproduction of TSM concentrations is observed among global and regional TSM algorithms.

References:

Deliverable # TN12: Satellite ocean color data validation, 2020.

Deliverable # TN14: Algorithms development, 2020.

Deliverable # TN17: Evaluation of new ocean color data,2020

Doerffer, R. and Schiller, H. (2007) The MERIS Case 2 Water Algorithm. International Journal of Remote Sensing, 28, 517-535, doi: 10.1080/01431160600821127

EUMETSAT, “Sentinel-3 OLCI Marine User Handbook,” EUM/OPSSEN3/MAN/17/907205, 2018

Morel, A., Gentili, B., Claustre, H., Babin, M., Bricaud, A., Ras, J., et al. (2007a).Optical properties of the "clearest" natural waters. Limnology and Oceanography, 52, 217-229.